

Materials Research Express



PAPER

Characterization, antibacterial, and neurotoxic effect of Green synthesized nanosilver using *Ziziphus spina Christi* aqueous leaf extract collected from Riyadh, Saudi Arabia

RECEIVED

4 January 2018

REVISED


8 February 2018

ACCEPTED FOR PUBLICATION

14 February 2018

PUBLISHED

28 February 2018

Afaf El-Ansary¹, Arjumand Warsy¹, Maha Daghestani¹, Nada M Merghani¹, Abeer Al-Dbass², Wadha Bukhari¹, Badryah Al-Ojayan¹, Eiman M Ibrahim¹, Asma M Al-Qahtani¹ and Ramesa Shafi Bhat² 

¹ Central Laboratory, Female Center for Medical Studies and Scientific section, King Saud University, Riyadh, KSA, Saudi Arabia

² Biochemistry Department, College of Science, King Saud University, PO Box 22452, Zip code 11495, Riyadh, Saudi Arabia

E-mail: rbhat@ksu.edu.sa

Keywords: nanosilver, *Ziziphus spina Christi*, antibacterial

Abstract

The current study aims to synthesize silver nanoparticles using *Ziziphus spina Christi* (ZSC) or (Sidr) aqueous leaf extract collected from Riyadh, Saudi Arabia. The green synthesis of silver nanoparticles using sidr leaves extract was successful. Production of silver nanoparticles was confirmed through UV–vis Spectrophotometer, particles size and zeta potential analysis, Infra-red spectroscopy, Scanning, and Transmission Electron Microscope (SEM and TEM). The UV–visible spectra showed that the absorption peak existed at 400 nm. SEM analysis showed that the synthesized AgNPs were spherical but in slightly aggregated form. TEM demonstrated different size range of 4–33 nm with an average size of 13. The element analysis profile showed silver signal together with oxygen, calcium, and potassium peaks which might be related to the plant structure. Biological effects of the synthesized AgNPs exhibit satisfactory inhibitory effect against ten tested microorganisms. It inhibited the growth of 5 gram-positive and five gram-negative bacteria. Moreover, AgNPs demonstrated a synergistic effect on the neurotoxicity induced in rat pups with orally administered methyl mercury (MeHg). The present study showed that AgNPs prepared from ZSC might be a promising antimicrobial agent for successful treatment of bacterial infection in intensive care units (ICU) especially in case of antibiotic resistance.

1. Introduction

Since the advent of nanotechnology, numerous physical techniques have emerged to synthesize nanoparticles, including sol-gel, ion sputtering, and chemical reductions [1–3]. However, lately, an interesting trend, known as green synthesis or biological synthesis of nanoparticles, has emerged [4] and several green leaves from different plants have been used for this purpose. In comparison to the conventional methods of nanoparticle synthesis, green biosynthesis has gained considerable attention and is recommended, as it has less impact on the environment with minimizing or no health hazards [5].

Nanosilver (nanoAg) usually occurs in the form of suspension which consists of particles of size less than 100 nm. These particles are traditionally used in many applications, including textiles, as conductive materials and most commonly in medical devices. Relative to the popularity of nanoAg and its growing applications, a considerable increase in the number of people occupationally exposed to these particles has also been observed. Due to antimicrobial activity, Ag NPs are suitable for a variety of applications like drug delivery systems, sanitization, water treatment, and wound healing [6–11]. It is well known that the biological activity and ability to cross the blood-brain barrier is related to the size and surface coating of the nanoAg [12]. It has been reported that translocation of nanoAg with average size 10–75 nm through barrier cells takes place at different rates, ranging from 30 min to 3 h without disrupting the tight junctions of the brain. Since nanoAg can be absorbed through the lungs, intestine, and skin into blood, it may reach different organs. In the few years, a number of

studies have been published in an attempt to understand various aspects of the toxicity of nanosilver [13–15]. Moreover; nanoAg may induce neurotoxicity which in turn can impair cognitive functions [16].

In several studies, different plants have been used for the synthesis of nanoAg. These include *Ziziphus jujuba*, a plant locally grown in Saudi Arabia and used extensively for its health benefits. The medicinal properties of Ziziphus tree, also known as nabq or sidr, were also recognized and have been in use in Pharaonic carpentry, diet, and medicine. The Quran mentions the sidr tree twice and accordingly it is highly respected by the Muslims throughout the Middle East [17]. It is traditionally used in the Muslim countries to wash the bodies of dead Muslims prior to burial, with water in which *Ziziphus jujuba* leaves had been soaked [18]. Leaves of *Ziziphus jujuba* contain a compound known as Ziziphin which demonstrates medicinal properties and is commonly used in traditional medicine. Among the medicinal properties of Ziziphus jujube are sedative properties, anticancer, antioxidants, antimicrobial and anti-inflammatory effects [19, 20]. The *Ziziphus jujuba* plant is rich in several organic compounds, including phenolic compounds, alpha-tocopherol, and beta-carotene. Besides these, alkaloids, flavonoids, sterols, tannins, saponin, and fatty acids have also been encountered in different species of the genus Ziziphus [21–24]. A few studies attempted to synthesize nanoAg using the leaves of *Ziziphus jujuba* plant, but the nanoAg prepared from plants grown in different regions of Saudi Arabia showed different characteristics [25, 26]. At the biological level, a recent study indicates that limited tissue distribution of silver detected from AgNPs is due to AgNP dissolution to silver ion. AgNPs, therefore, demonstrate adequate safety through limited penetration and absorption especially when given as intranasal drops [27]. It is well documented that all silver nanomaterials coated with different materials (e.g., plant organic compounds) are 3–10 times less toxic to than AgNO₃ [28] thus, the toxicity of silver nanomaterials depends on how efficiently silver ions are released from the nanomaterials. This information raised our interest to synthesize nanoAg from the water extract of *Ziziphus jujuba*, in an attempt to further use the medicinal properties of this plant. In this paper, we present the characteristics of biologically prepared nanoAg from *Ziziphus jujuba* and compare the antibacterial and toxicity properties of nanoAg compared to the water extract of the plant.

2. Material and methods

2.1. Preparation of leaf extract

Fresh and healthy leaves of *Ziziphus jujuba* were collected from Riyadh during November. The leaves were washed thoroughly with running water from the tap, followed with double distilled water and were later air dried at room temperature. After complete removal of the debris and other contaminating organic materials, the cleaned leaves were chopped and grounded, and 20 g was placed in a beaker containing 200 ml of doubled distilled water. The mixture was boiled over a flame for almost 30 min, cooled to room temperature and filtered through Whatman No 1 filter paper, to obtain a clear filtrate. The filtrate was stored at 4 °C until required for further analysis.

2.2. Green synthesis of silver nanoparticles

To the freshly prepared leaf extract, an aqueous solution of silver nitrate AgNO₃ (2 mM) was added, to a final concentration of silver nitrate of 1 mM and this catalyzed the reduction of Ag⁺ ions. The reduction was monitored by following the color change of the reactants from faint light green to dark brown (figure 1(A)). Time and color change were recorded, along with periodic sampling and scanning by UV–visible spectrophotometer, for a maximum of 5 h. Suitable controls were maintained throughout the experiment.

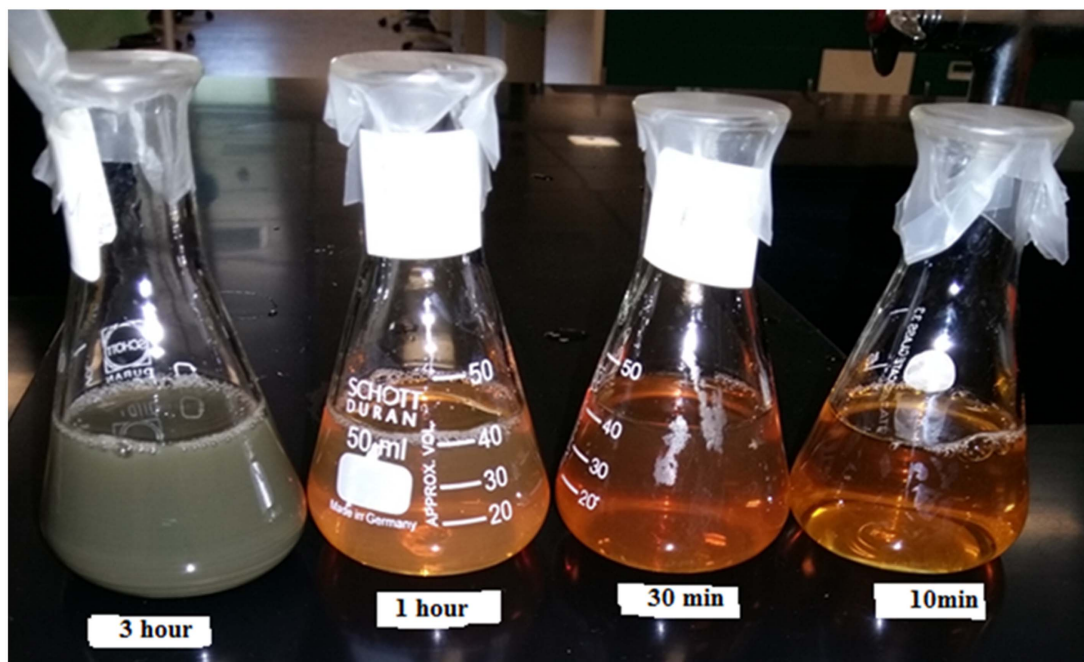
2.3. Characterization techniques

The synthesized leaf extract nanoAg particles were characterized using different techniques:

2.4. UV–vis spectra analysis

UV/Vis spectroscopic analysis was performed as one of the easiest and quick approaches for detection and characterization of AgNP [27]. The UV–vis absorbance spectra indicated that nanoAg could shift the absorption maximum to the visible light region [29]. Samples (1 ml) of the suspension were collected periodically to monitor the completion of bioreduction of Ag⁺ in aqueous solution by scanning in UV–visible (vis) spectra. The spectral analyses were conducted by recording the absorbance at the wavelengths from 300 to 600 nm in a UV–vis spectrophotometer. The recording was carried out periodically at intervals of 10 min, 30 min, 60 min and 3 Average sizes of the synthesized nanosilver.

A



B

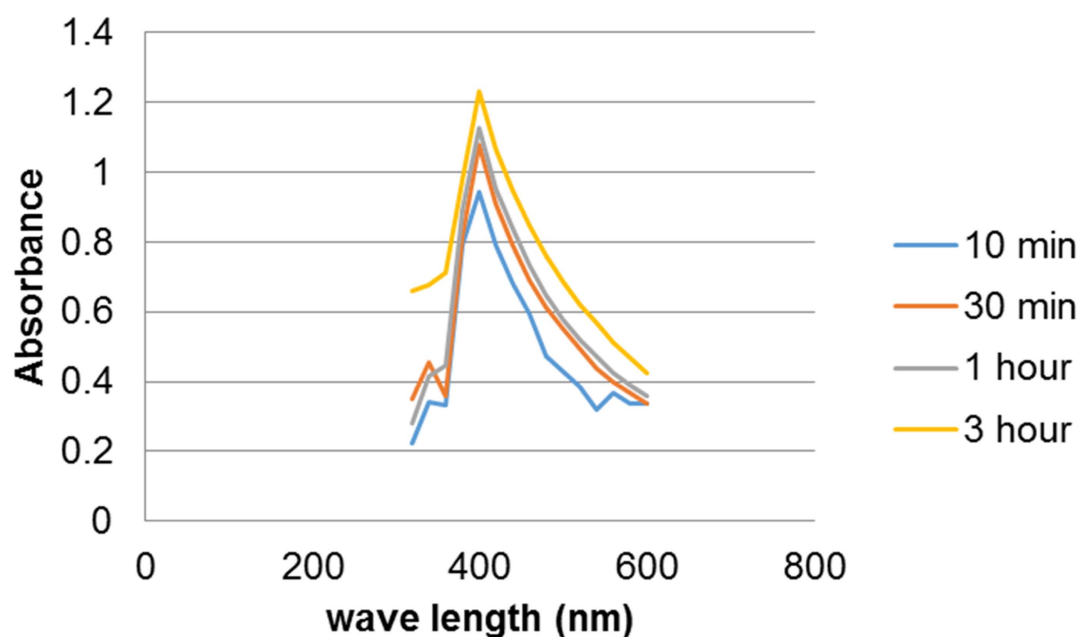


Figure 1. A; Color change, B; UV-Vis spectra showing absorbance with (different time intervals) with silver nanoparticle from ZSC leaves extract (50 mg ml^{-1}).

2.5. Average size of the synthesized nanosilver

2.5.1. Transmission Electron Microscopy (TEM)

The prepared nanoAg particles were subjected to the determination of the average particle size, using transmission electron microscope (TEM). Transmission Electron Microscopy (TEM) is an excellent technique, widely applied for particle sizing. It helps sample imaging on the absorption of a beam of electrons, during its passage through an ultrathin sample (Less than 100 nm). The transmitted beam is then projected onto a detector, which enables the visualization of objects in the nanometer-sized range.

2.5.2. Particles size and zeta potential analysis

The hydrodynamic size of nanoAg particles and Zeta potential were measured in the nanoAg solution by Zetasizer Nano Series ZS, Model number: ZEN3600. This instrument measures particle size by illuminating the particles with a 633 nm wavelength red laser, at a scattering angle of 173° , a measurement temperature of 25°C , and a medium viscosity of 0.887 mPa s. Zeta potential value helps in understanding the inter-particle interaction forces. The importance of zeta potential value can be related to the stability of colloidal dispersions. Particles in the suspension with low density and smaller sizes with a large negative or positive zeta potential repel each other, and the system is relatively stable and resists aggregation.

2.5.3. Infra-red spectroscopy (IR)

Infrared spectroscopy is usually used to detect the nature of bio-reducing functional groups, adsorbed molecules at the surface of synthesized NPs and the changes related to the surface chemistry [30]. Infra-red spectroscopy of the synthesized nanoAg was carried out in our central laboratory, KSU, Riyadh, Saudi Arabia.

2.6. Estimation of antibacterial activity

The antibacterial activity of the nanoAg particles and the plant leaf extracts were tested against ten strains of Gram (+) ve and Gram (–) ve bacteria. These included: *Staphylococcus aureus*, *Staphylococcus epidermis*, *Bacillus subtilis*, *Streptococcus pneumonia*, *Enterococcus faecalis*, *Escherichia coli*, *Salmonella typhi*, *Pseudomonas aeruginosa*, *Klebsiella pneumonia* and *Providencia stuartii*. For testing the plant leaf extract and the nanoAg particles containing solutions, the Disc diffusion method was applied. The discs were soaked with 100 μl of double distilled water, silver nitrate (+control), and nanoAg particle solution, separately and were air dried under sterile conditions. The plates containing nutrient agar media aureus and by swabbing them with the microbial cultures. The plates with the media and the cultures were divided into four equal parts, and previously prepared discs were placed on each part of the plate. The plates were incubated at 37°C for 16 h. At the end of the incubation period, the maximum zone of inhibition was observed and measured for analysis against each type of microorganism.

2.7. Neurotoxic effect

Twenty-eight Male Western albino rats (100–150 g) were obtained from King Saud University Riyadh and divided into four groups with seven rats in each group. The animals were kept under standard conditions of temperature and humidity. The control group (Group 1) received phosphate buffered saline throughout the experiment. Group 2 was given chronic dose of methyl mercury [CH_3Hg] (0.5 mg/kg/BW) for 21 days. T Group 3 received the same dose of CH_3Hg followed by a 1 ml dose of plant extract for one month and Group 4 also received the same dose of CH_3Hg followed by the 1 ml of nanosilver for one month.

2.7.1. Ethics approval

All animal experiments were conducted after receiving ethical approval from the Ethical Committee at King Saud University, Riyadh, Saudi Arabia.

Brain tissue was collected and washed with normal cold saline and then homogenized in ten volume/weight of distal water. The homogenate was then centrifuged at 3000 rpm for 10 min. The supernatant obtained was used for lipid oxidation and glutathione estimation by the method of Ruiz-Larrea *et al* [31] and Beutler *et al* [32], respectively.

3. Results and discussion

Nanosilver has attracted attention since the fourth century AD, due to the dichroic character when it is integrated into the glass [33]. More recently; silver was incorporated into different materials to increase durability and other properties [34]. At a certain size, the silver becomes colorless, and it makes more chemically durable materials, which slowly release silver ion for an extended period. Such materials are highly desirable for medical and dental applications, in cosmetics, plastics, soaps, pastes, food and textiles, and food containers [34]. Interestingly, the mention of transparent silver goes far back, when almost 1400 years ago, the Holy Quran mentions the existence of goblets made of silver but transparent like glass (Holy Quran chapter 76, verses 15–16). Since properties of NPs change, as the transformation occurs from the bulk material with decreasing particle size to nano size. Metals as silver, which are opaque may change to transparent.

We report here a fast, inexpensive and reproducible procedure for the synthesis of nanoAg particles. The addition of aqueous extract of ZSC leaves into an aqueous solution of silver nitrate (1 mM) led to the formation of nanoAg particles. This process could be easily visualized and monitored through the change of color of the reaction solution from faint light green to brown. Figure 1 presents the UV spectra of AgNPs obtained at

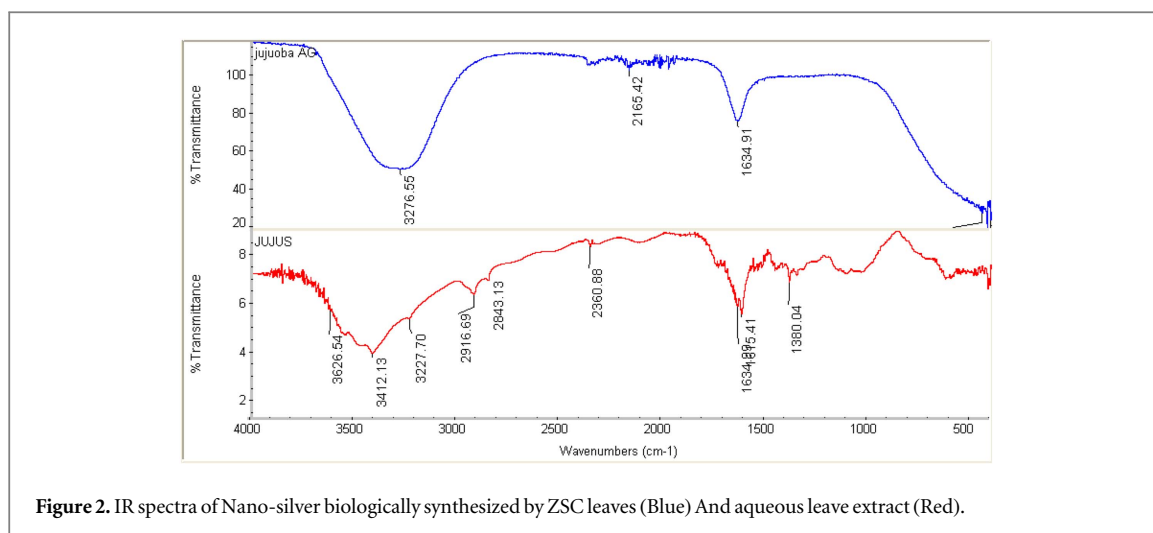
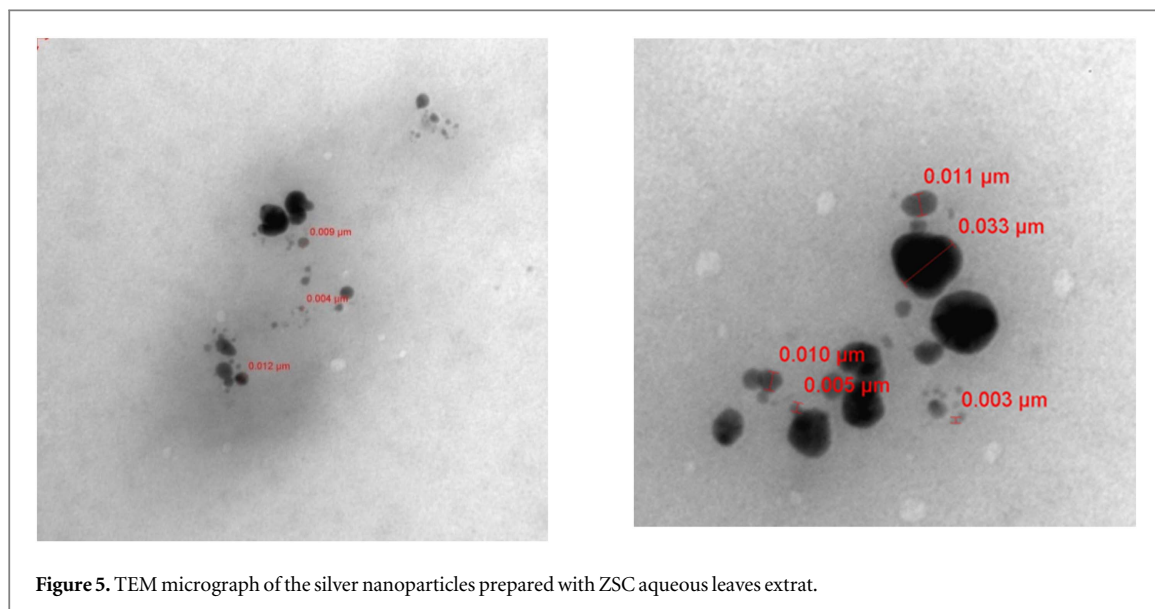
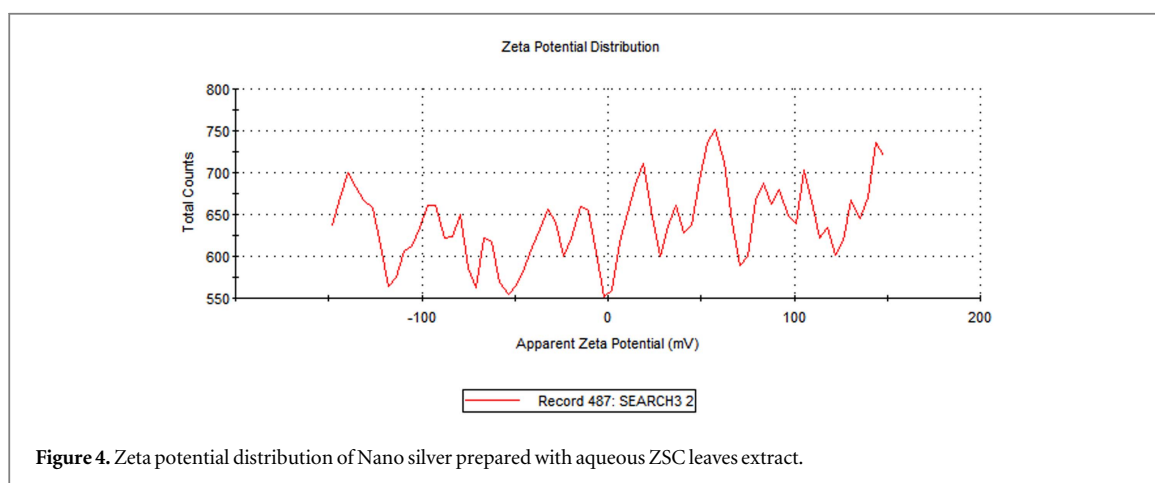
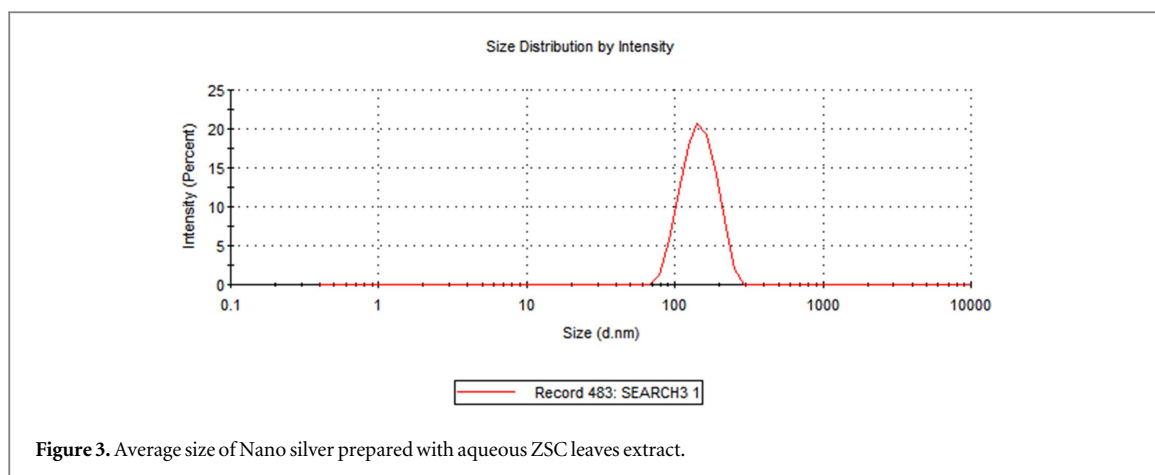


Figure 2. IR spectra of Nano-silver biologically synthesized by ZSC leaves (Blue) And aqueous leaf extract (Red).

different durations. The spectra generated by the nanoparticles was recorded after different time intervals of 10 min, 30 min, 1 h, 3 h, from the initiation of reaction using one mM solution of AgNO_3 and the same amount of plant extract. The results demonstrated a constant maximum absorption at 400 nm reflecting controlled size and shape of the synthesized nanoparticles in the aqueous solution of ZSC. There was a direct relationship between the time interval and the yield of AgNPs. These findings are in good agreement with the results of a recent study published by Ahmed *et al* [35], who recorded time as a factor influencing the yield of nanoAg particles from *Azadirachta indica* aqueous leaf extract. Moreover, the maximum spectrum band obtained at 400 nm is comparable to that recorded for nanoAg particles synthesized from *Zizyphus spina Christi* collected from Taif, KSA, and slightly different from that recorded for AgNPs biologically synthesized from *Zizyphus jujuba* leaf extract with absorption band centered at λ maximum at 434 nm. These findings reflect surface plasmon resonance (SPR) of the green synthesized AgNPs [26].

It is well known, that green synthesis of NP takes place through three levels which are: activation phase, growth phase, and termination phase. In the primary activation phase, the metal ions are separated from their salt under the effect of plant metabolites and biomolecules that possess reduction capabilities and that reduce the metal ions from divalent to zero-valent states. During the growth phase, the separated reduced metal atoms combine to form NPs while more biological reduction takes place. Finally, the termination phase was attained during which the NPs reached their stable morphology and were capped by plant metabolites [36–38]. The IR spectrum of green synthesized AgNPs showed an intensive peak at 1634.91 cm^{-1} , 2165.92 cm^{-1} , and 3256.55 cm^{-1} (figure 2), which deviated slightly from those recorded by Halawani *et al* [26] for *Zizyphus spina christi* collected from Taif. The peaks with strong absorption at 3276.55 cm^{-1} were attributed to the stretching of the hydroxyl groups, as a functional group of carbohydrates, phenols, flavonoids, and alcohols, while the peak at 1634.91 was assigned for the C=O stretching (carboxylic or amide) and C=C bond [39]. In the present study, the less intense peak at 1380.80 cm^{-1} representing carboxyl groups, previously reported by Halawani *et al* [26] suggests that the phytochemical composition of ZSC can vary from region to region with different environmental factors and climate. The additional peaks recorded at 1727.222 and 1075.71 cm^{-1} in the AgNPs synthesized by Halawani *et al* [26] were missing in the IR spectra of the nanoAg synthesized during the present study. This finding supports the suggestion made in the previous studies which show that differences of biomolecules in plants affect the biosynthesis of nanoparticles [40]. It is well known that high amount of phenolic compounds in the plant extract usually influence the reduction process and stabilization of nanoparticles [40]. Based on this we can suggest that hydroxyl, amino, carbonyl and amide moieties in the ZSC extract were effective in the reduction and stabilization of the synthesized NPs. Plants grown under different environmental conditions differ in the composition of these organic metabolites and hence show differences in the characteristics of the nanoAg produced from them biologically [41]. Using TEM as an analytical tool, the synthesized AgNPs demonstrates less aggregation and are spherical with size ranging from 4 to 33 nm in diameter with an average size of 13 nm (figure 6). The range of AgNPs size and the average size obtained in the present study was much lower than those reported by Halawani *et al* [26]. They reported a higher average size of the produced AgNPs, ranging in size from 21.5 to 59.67 nm. The average NPs size obtained in the present study was more or less similar to that previously produced from the same plant species in Egypt [26].

In the present study, the remarkably larger nanoAg size recorded by Zetasizer (ZS) (117 nm) (figures 3 and 4), compared to the size measured by TEM (average size 13 nm, and largest recorded size, 33 nm) can be attributed to the fact that TEM measures a number based size distribution of the physical size only, not including the



hydrodynamic status or mass-based size distribution. However, ZS is very sensitive to small amounts of large particles either due to aggregation or contamination [42], and this can be the reason for shifting the ZS measured particles to larger sizes. What the six-fold larger size of AgNPs found in our results by ZS finds agrees with the results of a previous study of Souza *et al* [43] in which almost the same difference was reported.

According to the SEM micrograph, the morphology of the synthesized AgNPs was spherical but was in slightly aggregated form. The agglomeration of small AgNPs shown by SEM micrograph can be confirmed through the remarkably smaller size recorded by TEM (figure 6).

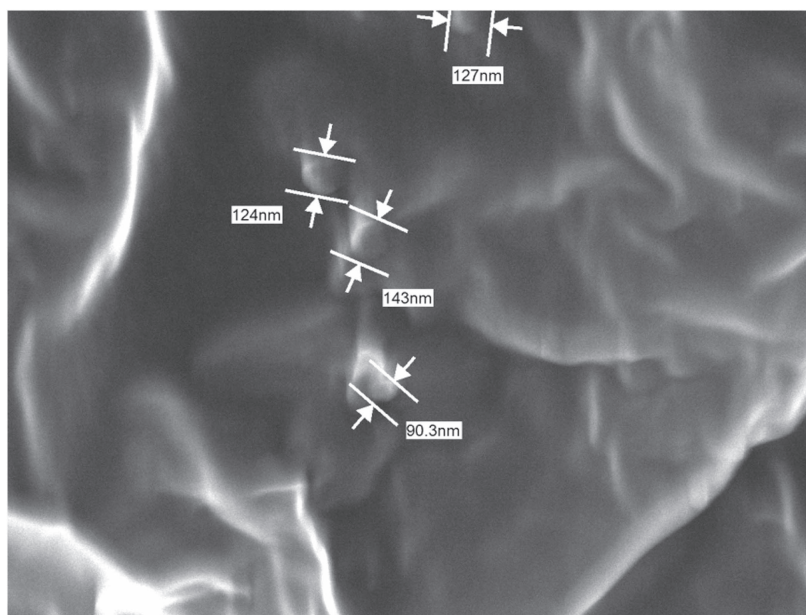


Figure 6. SEM micrograph of the AgNPs prepared with aqueous ZSC aqueous leaves extract.

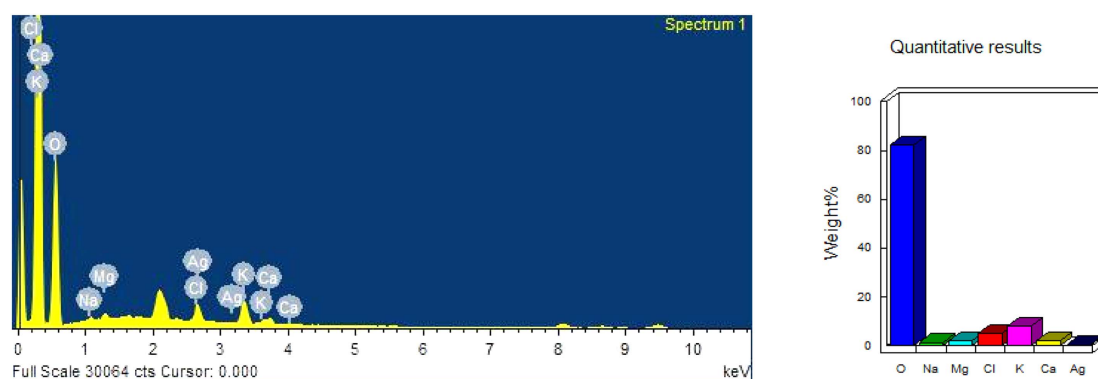
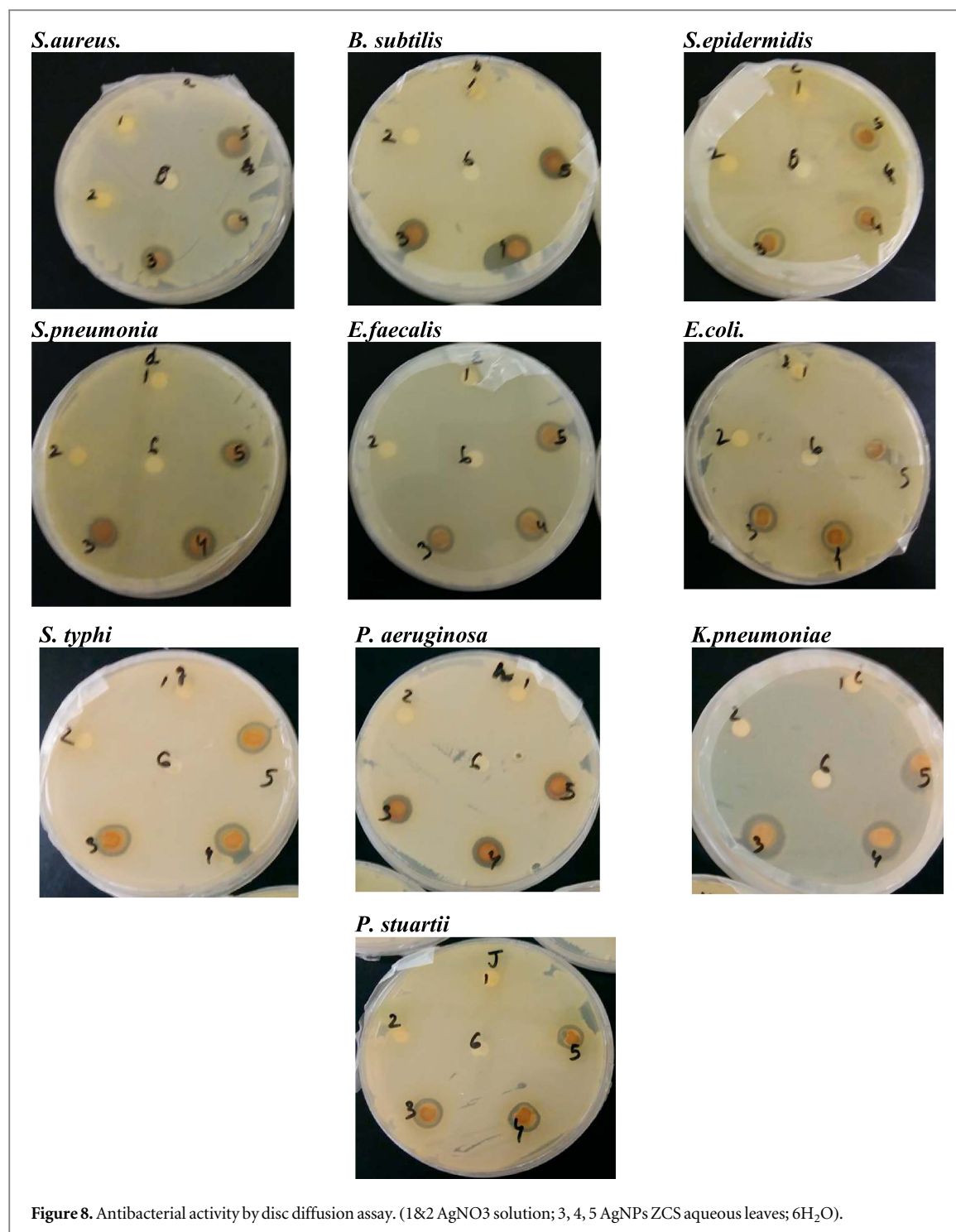


Figure 7. EDX elemental analysis of the AgNPs prepared with aqueous ZSC aqueous leaves extract.

Table 1. Antibacterial activity of biosynthesized AgNPs ZCS aqueous leaves extract against bacterial species tested by disc diffusion assay.

	Strains	Zone of Inhibition (mm)
Gram +ive	<i>S.aureus.</i>	15 ± 0.50
	<i>B. subtilis</i>	12 ± 0.30
	<i>S.epidermidis</i>	14 ± 0.70
	<i>S.pneumonia</i>	14 ± 0.10
	<i>E.faecalis</i>	14 ± 0.50
Gram –ive	<i>E.coli.</i>	12 ± 0.50
	<i>S. typhi</i>	13 ± 0.40
	<i>P. aeruginosa</i>	16 ± 0.30
	<i>K.pneumoniae</i>	12 ± 0.10
	<i>P. stuartii</i>	13 ± 0.10

The EDS elemental analysis of AgNPs presented in figure 7 shows Ag peaks which confirm that the pellets are silver nanoparticles. EDS profile shows weak silver signal together with remarkably stronger oxygen, calcium, and potassium peaks. These elements may originate from the plant biomolecules that are bound to the surface of the AgNPs. This suggestion can be explained based on the results of the previous work [44] in which they



reported that green synthesized nanoparticles using plant extracts are surrounded by a thin layer of some capping organic substances from the plant leaf, as seen in the TEM micrograph. SEM shows characteristic silver peaks on the surface of nanoparticles, suggesting that AgNPs are successfully synthesized using ZSC.

Ten different bacterial strains were tested for antibacterial activity of the nanoAg prepared from aqueous ZSC leave extract. The results showed that nanoAg inhibited the growth of all the gram -ve and gram +ve bacteria as shown in table 1 and figure 8. Among the Gram +ve, *S. epidermidis*, and *S. pneumonia* were the most sensitive to the AgNPs followed by *S. aureus*, and *E. faecalis* recording 14, 13 and 12 mm inhibition ring, respectively. Regarding the Gram-negative bacteria, *S. typhi* was the most sensitive (13 mm), while *K. pneumoniae* and *P. stuartii* were less sensitive (10 mm). Based on results, it was confirmed that the AgNPs were effective antibacterial agents against some bacteria. These results are in agreement to those obtained for the AgNPs prepared from the ZSC leave extract collected from Najran, Saudi Arabia and tested against five out of the eleven strains tested in the present study [45]. Interestingly, *S. epidermis* and *Enterococcus faecalis* are the two

Table 2. Effect of biosynthesized AgNPs prepared and aqueous ZSC extract against methyl mercury-induced neurotoxicity in rat pups.

Parameter	Group	Mea±S.D.	Pvalue ^a
Lipid peroxidase	Control	0.22 ± 0.00	0.699
	CH ₃ Hg treated	0.33 ± 0.02	
	CH ₃ Hg+extract	0.45 ± 0.03	
	CH ₃ Hg+nano extract	0.55 ± 0.02	
GSH	Control	24.75 ± 0.2	0.767
	CH ₃ Hg treated	14.66 ± 1.25	
	CH ₃ Hg+extract	20.55 ± 3.6	
	CH ₃ Hg+nano extract	22.94 ± 3.66	

^a P value between control group and other groups.

major bacterial strains that colonize in the central venous catheters and are a significant cause of catheter-related bloodstream infections. As shown in this study, the green synthesized AgNPs can be used to reduce the catheter-related infections. These infections are usually associated with high rate of health care costs, morbidity, and [46–49]. As *S. aureus* and *S. pneumoniae* colonize in the patients admitted to the intensive care unit and increase the risk to develop pneumonia almost 15 folds, a practical application can be to sterilize ICU equipment using green synthesized nanosilver. Such sterilization strategies may play a significant role in decreasing the prevalence of *S. pneumoniae* infections in the ICU [50]. Moreover, the antibacterial effect of the synthesized AgNPs against *S. typhi* may be effective in reducing soft tissue infections, and abscesses, especially in immunocompetent patients admitted to ICU [51]. Ventilator-associated pneumonia (VAP) was recognized as the most common infections in the ICU of many hospitals and *K. pneumonia*, *P. aeruginosa* were identified as bacterial strains contributing to the etiology of VAP [52–54]. Since the nanoAg synthesized during this study was effective against both the bacterial strains, we suggest that the use of nanoAg may help in reducing the growth of these bacterial and hence VAP. Moreover, in the burns unit, the overgrowth of *P. stuartii* is commonly encountered. This infection can be reduced through the use of AgNPs, particularly in cases of antibiotic resistance developed by this bacterial strain [55].

In a study conducted at King Khalid Hospital, Hafr Al-Batin, Saudi Arabia, *E. coli*, *K. pneumonia*, and *P. aeruginosa* were reported as the Gram-negative bacteria that develop resistance to antibiotic treatment. The most common antibiotic-resistant bacteria were found in the female surgical ward (100%) followed by ICU (90.2%), and male surgical ward (88.2%). The *S. aureus* was the only Gram-positive strain that developed 100% antibiotic resistance, *K. pneumonia* was 93.3% antibiotic resistance, *E. coli* developed 75.7%, and *P. aeruginosa* 100%. Among the different antibiotics, *S. aureus* showed high resistance to ampicillin and linezolid (94.1%). High (86.95%) and complete resistance (100%) against ampicillin were observed in *E. coli* and *K. pneumonia*, respectively. *P. aeruginosa* was fully resistant to 4 antibiotics, i.e., cefazoline, cefoxitin, tetracycline, and trimethoprim-sulfamethoxazole [56]. Table 2 presents the toxic effect of green synthesized AgNPs. It can be noticed that nanoAg shows a synergistic effect on the neurotoxicity induced in rat pups brain with orally administered methyl mercury (MeHg). AgNPs/MeHg induced a much higher increase of lipid peroxides as a marker of oxidative stress compared to MeHg intoxication and of course much higher when compared with healthy control animals. On the other hand, both plant extract and AgNPs plant extract induced a remarkable increase of GSH level in treated rat brain which can be attributed to the high content of GSH in ZSC [57]. These results are in agreement with the previous study of Liu [58] in which they reported that intranasal administration of AgNPs to rats induced accumulation of reactive oxygen species (ROS) in tissue homogenate of the hippocampus leading to oxidative DNA damage, neuroinflammation, and apoptosis. This can find support in the most recent study of Ema [59], in which they reported that exposure of maternal rats to oral AgNPs (20 nm) and suggested that it causes oxidative stress, which consequently leads to apoptosis and neuronal death in the brain of offspring. Brain dysfunction in AgNPs-treated exposed rat pups was accompanied by impaired cognitive behaviors together with delayed physical development [59].

4. In conclusion

The present study demonstrates the antibacterial effectiveness of the green synthesized AgNPs against multiple pathogenic microbes. However, the controvert obtained regarding its neurotoxic effect (increase both lipid peroxides and GSH) needs to be verified.

Competing interests

The authors declare that they have no competing interests.

Acknowledgments

This research project was supported by a grant from the research center of the Center for Female Scientific and Medical Colleges at King Saud University

ORCID iDs

Ramesa Shafi Bhat  <https://orcid.org/0000-0003-2149-6239>

References

- [1] Bindhu M R and Umadevi M 2015 Antibacterial and catalytic activities of green synthesized silver nanoparticles *Spectrochim Acta A Mol Biomol Spectrosc.* **135** 373
- [2] Pourmortazavi S M, Taghdiri M, Makari V and Rahimi-Nasrabadi M 2015 Procedure optimization for green synthesis of silver nanoparticles by aqueous extract of Eucalyptus oleosa *Spectrochim Acta A Mol Biomol Spectrosc.* **136** 1249
- [3] Rathi Sre P R, Reka M, Poovazhagi R, Arul Kumar M and Murugesan K 2015 Antibacterial and cytotoxic effect of biologically synthesized silver nanoparticles using aqueous root extract of Erythrina indica lam *Spectrochim Acta A Mol Biomol Spectrosc.* **135** 1137–44
- [4] Thuesombat P, Hannongbua S, Akasit S and Chadchawan S 2014 Effect of silver nanoparticles on rice (*Oryza sativa* L. cv. KDML 105) seed germination and seedling growth *Ecotoxicol Environ Saf* **104** 302–9
- [5] Tripathy A, Raichur A M, Chandrasekaran N, Prathna T C and Mukherjee A 2010 Process variables in biomimetic synthesis of silver nanoparticles by aqueous extract of *Azadirachta indica* (Neem) leaves *J. Nanopart Res* **12** 237–46
- [6] Judith Vijaya J, Jayaprakash N, Kombaiiah K, Kaviyarasu K, John Kennedy L, Jothi Ramalingam R, Al-Lohedan H A, Mansoor Ali V M and Maaza M 2017 Bioreduction potentials of dried root of Zingiber officinale for a simple green synthesis of silver nanoparticles: Antibacterial studies *J. Photochem. Photobiol. B* **177** 62–8
- [7] Jayaprakash N, Vijaya J J, Kaviyarasu K, Kombaiiah K, Kennedy L J, Ramalingam R J, Munusamy M A and Al-Lohedan H A 2017 Green synthesis of Ag nanoparticles using Tamarind fruit extract for the antibacterial studies *J. Photochem. Photobiol. B* **169** 178–85
- [8] Kaviyarasu K et al Elucidation of photocatalysis, photoluminescence and antibacterial studies of ZnO thin films by spin coating method *J. Photochem. Photobiol. B* 2017 **173** 466–75
- [9] Magdalane C M, Kaviyarasu K, Vijaya J J, Siddhardha B and Jeyaraj B 2016 Photocatalytic activity of binary metal oxide nanocomposites of CeO₂/CdO nanospheres: investigation of optical and antimicrobial activity *J. Photochem. Photobiol. B* **163** 77–86
- [10] Kaviyarasu K, Mariappan A, Neyvasagam K, Ayeshamariam A, Pandi P, Rajeshwara R, Palanichamy P, Gopinathan C, Genene T M and Maaza M 2017 Photocatalytic performance and antimicrobial activities of HAp-TiO₂ nanocomposite thin films by sol-gel method *Surfaces and Interfaces* **6** 247–55
- [11] Anand K, Kaviyarasu K, Muniyasamy S, Roopan S M, Gengan R M and Chuturgoon A A 2017 Bio-synthesis of silver nanoparticles using agroforestry residue and their catalytic degradation for sustainable waste management *J. Cluster Sci.* **28** 2279–91
- [12] Gonzalez-Carter D A, Leo B F, Ruenraroengsak P, Chen S, Goode A E, Theodorou I G, Chung K F, Carzaniga R, Shaffer M S, Dexter D T, Ryan M P and Porter A E 2017 Silver nanoparticles reduce brain inflammation and related neurotoxicity through induction of H₂S-synthesizing enzymes *Sci. Rep.* **7** 42871
- [13] Ezhilarasi A A, Vijaya J J, Kaviyarasu K, Maaza M, Ayeshamariam A and Kennedy L J 2016 Green synthesis of NiO nanoparticles using Moringa oleifera extract and their biomedical applications: Cytotoxicity effect of nanoparticles against HT-29 cancer cells *J. Photochem. Photobiol. B* **164** 352–60
- [14] Kaviyarasu K, Kanimozhi K, Matinise N, Maria Magdalane C, Mola G T, Kennedy J and Maaza M 2017 Antiproliferative effects on human lung cell lines A549 activity of cadmium selenide nanoparticles extracted from cytotoxic effects: investigation of bio-electronic application *Mater Sci Eng C Mater Biol Appl.* **1** 1012–25
- [15] Kaviyarasu K, Geetha N, Kanimozhi K, Maria Magdalane C, Sivaranjani S, Ayeshamariam A, Kennedy J and Maaza M 2017 *In vitro* cytotoxicity effect and antibacterial performance of human lung epithelial cells A549 activity of Zinc oxide doped TiO₂ nanocrystals: investigation of bio-medical application by chemical method *Mater. Sci. Eng. C Mater. Biol. Appl.* **74** 325–33
- [16] Liu Y, Guan W, Ren G and Yang Z 2012 The possible mechanism of silver nanoparticle impact on hippocampal synaptic plasticity and spatial cognition in rats *Toxicol. Lett.* **209** 227–231
- [17] Farooqi A 1997 Plants of the Qur'an (Lucknow (India): Sidrah Publishers) pp 65–74
- [18] Dafni A, Levy S and Lev E 2005 The ethnobotany of Christ's Thorn Jujube (*Ziziphus spina-christi*) in Israel *J. Ethnobiol Ethnomed.* **1** 8
- [19] Abdel-Zaher A O, Salim S Y, Assaf M H and Abdel-Hady R H 2014 Effect of silver nanoparticles on rice (*Oryza sativa* L. cv. KDML 105) seed germination and seedling growth *Ecotoxicol Environ Saf.* **104** 302–9
- [20] Li J W, Ding S D and Ding X L 2005 Comparison of antioxidant capacities of extracts from five cultivars of Chinese jujube *J. Process. Biochem.* **40** 3607
- [21] Zhao Z H, Liu M J and Tu P F 2008 J. Characterization of water soluble polysaccharides from organs of Chinese Jujube (*Ziziphus jujuba* Mill. cv. Dongzao) *Eur. Food Res. Technol.* **226** 985
- [22] Guil-Guerrero J L, Díaz Delgado A, Matallana González M C and Torija Isasa M E 2004 Fatty acids and carotenes in some ber (*Ziziphus jujuba* Mill) varieties *Plant Foods Hum. Nutr.* **59** 23
- [23] Pareek S 2013 Nutritional composition of jujube fruit *J. Food Agric* **25** 463
- [24] San B and Yildirim A N 2010 Phenolic, alpha-tocopherol, beta-carotene and fatty acid composition of four promising jujube (*Ziziphus jujuba* Miller) selections *Journal of Food Composition and Analysis* **23** 706–20
- [25] Masoud E A, A. Al-Hajry M and Al-Marrani A 2016 Antibacterial activity of silver nanoparticles synthesized by sidr (*Ziziphus spina-christi*) leaf extract against pathogenic bacteria *Int. J. Curr. Microbiol. App. Sci.* **5** 226

- [26] Halawani E M 2017 Rapid biosynthesis method and characterization of silver nanoparticles using zizyphus spina christi leaf extract and their antibacterial efficacy in therapeutic *Application Journal of Biomaterials and Nanobiotechnology* **8** 22
- [27] Falconer J L and Grainger D W 2018 *In vivo* comparisons of silver nanoparticle and silver ion transport after intranasal delivery in mice *J. Control. Release* **269** 1–9
- [28] Kwok K W, Auffan M, Badireddy A R, Nelson C M, Wiesner M R, Chilkoti A, Liu J, Marinakos S M and Hinton D E 2012 Uptake of silver nanoparticles and toxicity to early life stages of Japanese medaka (*Oryzias latipes*): effect of coating materials *Aquat. Toxicol.* **120–121** 59–66
- [29] Sikder M, Lead J R, Chandler G T and Baalousha M 2018 A rapid approach for measuring silver nanoparticle concentration and dissolution in seawater by UV–vis *Sci. Total Environ.* **618** 597–607
- [30] López-Lorente A I and Mizaikoff B 2016 Recent advances on the characterization of nanoparticles using infrared spectroscopy *Trends in Analytical Chemistry* **84** 97–106
- [31] Ruiz-Larrea M B, Leal A M, Liza M, Lacort M and de Groot H 1994 Antioxidant effects of estradiol and 2-hydroxyestradiol on iron-induced lipid peroxidation of rat liver microsome *Steroids*. **159** 383
- [32] Beutle E, Duran O and Kelly B M 1963 Improved method for the determination of blood glutathione *J. Lab Clin. Med.* **61** 882
- [33] Kawashita M, Tsuneyama S, Miyaji F, Kokubo T, Kozuka H and Yamamoto K 2000 Antibacterial silver-containing silica glass prepared by sol-gel method *Biomaterials* **21** 393–8
- [34] Karmakar B, Som T, Prakash Singh S and Nath M 2010 J. Nanometal-glass hybrid nanocomposites: synthesis, properties and applications *Transactions of the Indian Ceramic Society* **69** 171
- [35] Ahmed S, Ahmad M and Swami B L 2016 Green synthesis of silver nanoparticles using *Azadirachta indica* aqueous leaf extract *Journal of Radiation Research and Applied Science* **9** 1–7
- [36] Si S and Mandal T K 2007 Tryptophan-based peptides to synthesize gold and silver nanoparticles: a mechanistic and kinetic study *Chemistry* **13** 3160–8
- [37] Kim J, Rheem Y, Yoo B, Chong Y, Bozhilov K N, Kim D, Sadowsky M J, Hur H G and Myung N V 2010 Peptide-mediated shape- and size-tunable synthesis of gold nanostructures *Acta Biomater.* **6** 2681–9
- [38] Malik P, Shankar R, Malik V, Sharma N and Mukherjee T K 2014 Green chemistry based benign routes for nanoparticle synthesis *J. Nanopart.* **2014** 302429
- [39] Kummara S, Patil M B and Uriah T 2016 Synthesis, characterization, biocompatible and anticancer activity of green and chemically synthesized silver nanoparticles—A comparative study *Biomed Pharmacother.* **84** 10–21
- [40] Sathishkumar G, Gobinath C, Karpagam K, Hemamalini V, Premkumar K and Sivaramakrishnan S 2012 Phyto-synthesis of silver nanoscale particles using *Morinda citrifolia* L. and its inhibitory activity against human pathogens *Colloids Surf B Biointerfaces* **95** 235–40
- [41] Sampaio B L, Edrada-Ebel R and Da Costa F B 2016 Effect of the environment on the secondary metabolic profile of *Tithonia diversifolia*: a model for environmental metabolomics of plants *Sci. Rep.* **6** 29265
- [42] Baalousha M and Lead J R 2007 Size fractionation and characterization of natural aquatic colloids and nanoparticles *Sci. Total Environ.* **386** 93–102
- [43] Souza T G F, Ciminelli V S T and Mohallem N D S 2016 A comparison of TEM and DLS methods to characterize size distribution of ceramic nanoparticles *8th Brazilian Congress on Metrology (Metrologia 2015)* IOP Publishing, *Journal of Physics: Conf. Series* 733
- [44] Shankar S S, Rai A, Ahmad A and Sastry M 2004 Rapid synthesis of Au, Ag, and bimetallic Au core Ag shell nanoparticles using *Neem* (*Azadirachta indica*) leaf broth *J. Colloid Interface Sci.* **275** 496–502
- [45] Masoud E A, A. Al-Hajry M and Al-Marrani A 2016 Antibacterial activity of silver nanoparticles synthesized by *Sidr* (*Ziziphus spina-Christi*) leaf extract against pathogenic bacteria *Int. J. Curr. Microbiol. App. Sci.* **5** 226–36
- [46] Mermel L A, Farr B M, Sherertz R J, Raad I I, O'Grady N, Harris J A S and Craven D E 2001 Guidelines for the management of intravascular catheter-related infections *Clin. Infect. Dis* **32** 1249–72
- [47] Dimick J B, Pelz R K, Consunji R, Swoboda S M, Hendrix C W and Lipsett P A 2001 Increased resource use associated with catheter-related bloodstream infection in the surgical intensive care unit *Arch. Surg* **136** 229–34
- [48] Francolini I and Donelli G 2010 Prevention and control of biofilm-based medical-device-related infections *FEMS Immunol. Med. Microbiol.* **59** 227–38
- [49] Padmavathy K, Praveen S, Madhavan R, Krithika N and Kiruthiga A 2015 Clinico-microbiological investigation of catheter associated urinary tract infection by *enterococcus faecalis*: vanA Genotype *J. Clin. Diagn. Res.* **9** DD05–D06
- [50] Paling F P, Wolkewitz M, Bode L G M, Klein Klouwenberg P M C, Ong D S Y, Depuydt P, de Bus L, Sifakis F, Bonten M J M and Kluytmans J A J W 2017 *Staphylococcus aureus* colonization at ICU admission as a risk factor for developing *S. aureus* ICU. pneumonia *Clinical Microbiology and Infection* **23** e9–49
- [51] Sfeir M, Youssef P and Mokhbat J E 2013 *Salmonella typhi* sternal wound infection *Am. J. Infect. Control* **41** e123–4
- [52] Akhvlediani T, Akhvlediani N and Kuchuloria T 2016 Important aspect of health care associated infections in georgia with the focus on ventilator-associated pneumonia (review) *Georgian Med News* **258** 80–4
- [53] Yang Y W, Jiang Y Z, Hsu C M and Chen L W 2017 *Pseudomonas aeruginosa* ventilator-associated pneumonia induces lung injury through TNF- α /c-Jun NH2-terminal kinase pathways *PLoS One* **12** e0169267
- [54] Borgatta B, Lagunes L, Imbiscuso A T, Larrosa M N and Luján M 2017 Rello J Infections in intensive care unit adult patients harboring multidrug-resistant *Pseudomonas aeruginosa*: implications for prevention and therapy *Eur. J. Clin. Microbiol. Infect. Dis.* **36** 1097–104
- [55] Tran Q T, Mahendran K R, Hajjar E, Ceccarelli M, Davin-Regli A, Winterhalter M, Weingart H and Pagès J M 2010 Oct 15 Implication of porins in beta-lactam resistance of *Providencia stuartii* *J. Biol. Chem.* **285** 32273–81
- [56] Al Youssef S A 2016 Surveillance of Antibiotic-Resistant Bacteria in King Khalid Hospital, Hafr Al-Batin, Saudi Arabia, during 2013 *Jundishapur J. Microbiol.* **9** e19552
- [57] Mubarak M A, Hafiz T A, Al-Quraishy S and Dkhil M A 2017 Oxidative stress and genes regulation of cerebral malaria upon *Zizyphus spina-christi* treatment in a murine model *Microb Pathog.* **107** 69–74
- [58] Liu Y, Guan W, Ren G and Yang Z 2012 The possible mechanism of silver nanoparticle impact on hippocampal synaptic plasticity and spatial cognition in rats *Toxicology Letters* **209** 227–31
- [59] Ema M, Okud H, Gamo M and Honda K 2017 A review of reproductive and developmental toxicity of silver nanoparticles in laboratory animals *Reprod. Toxicol.* **67** 149–64